Purdue University
Purdue e-Pubs

International Compressor Engineering Conference   School of Mechanical Engineering

2012

Numerical Calculation and Analysis of Lubricating Water Film Cavitation of A Water Flooded Air Single Screw Compressor

Rui Huang
huangrui.6@stu.xjtu.edu.cn

Ting Li

Quanke Feng

Weifeng Wu

Follow this and additional works at: http://docs.lib.purdue.edu/icec

Numerical investigation of pressure distribution along the lubricating water film in water flooded air single screw compressors

Rui HUANG[1]*, Ting LI[1], Quanke FENG[1],Weifeng WU[1]

[1]School of Energy and Power Engineering, Xi'an Jiaotong University
Xi'an, 710049, China
86-29-82675258, Fax: 86-29-82663783, huangrui.6@stu.xjtu.edu.cn
* Corresponding Author

ABSTRACT

Reynolds equations and one-phase model with N-S (Navier Stocks) equations are widely used to calculate pressure distribution in the liquid film. In most cases, negative pressure exits in the obtained results. In a water-flooded single screw compressor, it is necessary to investigate the pressure of water film along the whole tooth flank. A negative pressure may not be right, because that when the pressure is lower than the saturated vapor pressure, cavitation occurs. In this paper, we investigated the pressure distribution of the water film with cavitation model. Results were compared to the pressure distribution obtained by one-phase model using N-S equations. Results show that difference of pressure distribution obtained by the two models is very similar for the positive pressure distribution. For the negative pressure distribution, the saturated vapor pressure could be applied to replace the results obtained by one-phase model with very small errors. Therefore, one-phase model will be effective to simulate pressure distribution along the tooth flank by using the vapor pressure to replace the negative pressure.

1. INTRODUCTION

Disadvantages of rapid wear of the star-wheel tooth in a single screw compressor (e.g., Zimmern, B., Patel, G. C.) have limited its development. As shown in Figure 1, clearance between the tooth flank and the groove is very small to seal compressed gas. During running, the tooth flank moves with a speed of 10~50m/s along the groove flank. Obviously, the tooth flank will be quickly worn if it contacts with the groove flank. Thus a perfect lubricating between the tooth flank and the groove flank could enhance the wear resistance of the tooth. Post and Zwaans(1986) (e.g., Post W., Zwaans M.) developed a simulation model to calculate the pressure distribution along the tooth flank and the groove flank. Double slider model were used to simulate the position of the tooth in the groove. Thus, it is necessary to investigate the pressure distribution of the lubricant along the both side of the tooth flank exactly. While using one phase model such as Reynolds equation, false negative pressure distribution exists in the results. For a water flooded single screw compressor, when the calculated pressure is lower than the saturated vapor pressure, it means cavitation may occur in these negative pressure zone. Therefore, pressure distribution obtained by one phase model maybe not true.
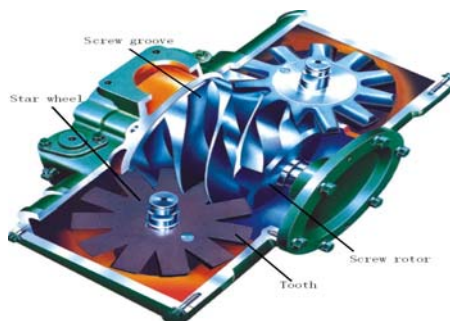

Figure 1: Basic components of a typical single screw compressor

In this paper, we investigated the pressure distribution of the water film along the tooth flank in the water flooded single screw compressor. Results obtained by using the cavitation model and the one-phase model were compared.

2. GEOMETRIC MODEL

To describe the geometric and kinematics relations between the screw rotor and the star wheel rotor, two right-handed Cartesian coordinates are introduced. As indicated in Figure 2, $S_1(X_1, Y_1, Z_1)$ and $S_2(X_2, Y_2, Z_2)$ coordinates are used for expressing the staring positions of the screw rotor and the star wheel rotor and thus are stationary, the origins O_1 and O_2 are chosen at the same horizontal plane, the Z_1-axis is in the axis of the screw rotor, and the Z_2-axis is the axis of the star wheel rotor. ϕ_2 is the rotation angle of the star wheel rotor around the Z_2-axes.
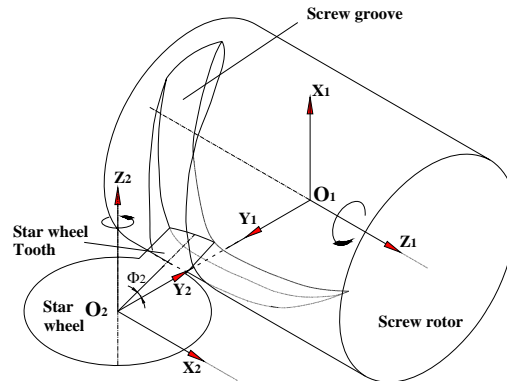
Figure 2: Schematic diagram of geometric and kinematic relations between the tooth and the groove
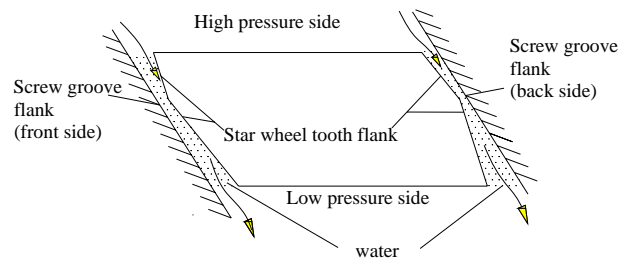
Figure 3: Schematic diagram of the meshing pair

As described in Figure 3，the screw rotor and the star wheel rotor mesh with each other during gas compressing. Water, as lubricating medium, is sprayed into the compression chamber. Under the action of the high pressure in the chamber and the relative sliding velocity of the two flanks, water is pressed into the gap.
We are concerned with the flow between the two surfaces as indicated in Figure 4. The screw groove(lower surface)flank moves with velocity U in the negative x direction, and the tooth flank(upper surface) is stationary. The clearance between the screw groove flank and the tooth flank h(x) is the function of x. Because of good cooling efficiency in water flooded single screw compressor, the compressing process can be seen as isothermal compression.
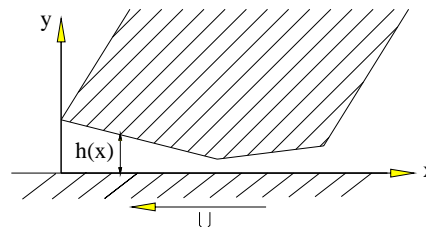
Figure 4: Geometrical configuration

3. PHYSICAL MODELS

In order to simply the physical model, we assume that the water pressure distribution does not change along the tooth length direction, and this can be seen as two-dimensional problem to study.

3.1 Mixture Model
The mixed gas-liquid two-phase flow is involved in this calculation, so it is necessary to use the Mixture multi-phase flow model.
The continuity equation (e.g., Junfu Wang) is given by

$$\frac{\partial}{\partial}(\rho m) + \nabla \cdot (\rho_m \vec{v}_m) = \dot{m} \tag{1}$$

where

$$\vec{v}_m = \frac{\sum_{k=1}^{n} \alpha_k \rho_k \vec{v}_k}{\rho_m} \tag{2}$$

$$\rho_m = \sum_{k=1}^{n} \alpha_k \rho_k \tag{3}$$

In the above equations, $\vec{v}_m$ is the mass-mean velocity, ρ_m is the density of the mixture, α_k is the volume fraction of the k phase, n is the number of phases, and $\dot{m}$ is the mass transfer caused by cavitation.
The momentum equation(e.g., Junfu Wang) of the mixture model is obtained from the sum of all the respective momentum equations. So, it can be expressed as:

$$\frac{\partial}{\partial t}(\rho_m \vec{v}_m) + \nabla \cdot (\rho_m \vec{v}_m \vec{v}_m) = -\nabla p + \nabla \cdot \left[\mu_m (\nabla \vec{v}_m + \nabla \vec{v}_m^T) \right] + \rho_m \vec{g} + \vec{F} + \nabla \cdot (\sum_{k=1}^{n} \alpha_k \rho_k \vec{v}_{dr,k} \vec{v}_{dr,k}) \tag{4}$$

Where
$\vec{F}$ is the body force of the flow, μ_m is the viscosity of the mixture, and $\vec{v}_{dr,k}$ is the sliding velocity of the k phase. μ_m and $\vec{v}_{dr,k}$ are respectively defined as

$$\mu_m = \sum_{k=1}^{n} \alpha_k \mu_k \tag{5}$$

$$\vec{v}_{dr,k} = \vec{v}_k - \vec{v}_m \tag{6}$$

Since there is no significant difference in velocity for the gas-liquid phases, there is no need to concern about the sliding velocity equation in this model. The gravity term is insignificant compared to others, so it is neglected too. The equation (4) is simplified as

$$\frac{\partial}{\partial t}(\rho_m \vec{v}_m) + \nabla \cdot (\rho_m \vec{v}_m \vec{v}_m) = -\nabla p + \nabla \cdot \left[\mu_m (\nabla \vec{v}_m + \nabla \vec{v}_m^T) \right] + \vec{F} \tag{7}$$

3.2 *k-epsilon* turbulence model
K-epsilon model is the most widely-used engineering turbulence model for industrial applications. The equations (e.g., Junfu Wang) include the continuity equation, the momentum equations and the k, e equations.
Continuity

$$\frac{\partial u}{\partial x} + \frac{\partial v}{\partial y} = 0 \tag{8}$$

Momentum

$$\frac{\partial}{\partial x_j}(\rho u_i u_j) = -\frac{\partial P}{\partial x_i} + \frac{\partial(\eta \frac{\partial u_i}{\partial x_j} - \rho \overline{u'_i u'_j})}{\partial x_j} \tag{9}$$

where

ρ is the density of the fluid, u is the mean velocity of turbulent flow, P is the flow pressure, η is the fluid dynamic viscosity, and $-\rho \overline{u'_i u'_j}$ is the turbulent stress.

k, e equations

$$\frac{\partial(\rho k)}{\partial t} + \frac{\partial(\rho k u_i)}{\partial x_i} = \frac{\partial}{\partial x_j}\left[(\mu + \frac{\mu_t}{\sigma_k})\frac{\partial k}{\partial x_j}\right] + G_k - \rho\varepsilon \tag{10}$$

$$\frac{\partial(\rho\varepsilon)}{\partial t} + \frac{\partial(\rho\varepsilon u_i)}{\partial x_i} = \frac{\partial}{\partial x_j}\left[(\mu + \frac{\mu_t}{\sigma_\varepsilon})\frac{\partial \varepsilon}{\partial x_j}\right] + \frac{G_{1\varepsilon}\varepsilon}{k}G_k - C_{2\varepsilon}\rho\frac{\varepsilon^2}{k} \tag{11}$$

Where

G_k is the turbulent kinetic energy caused by mean velocity gradient, C_1 and C_2 are constant, σ_k and σ_e are the turbulent Pr number.

3.3 Parameter setting

In this paper, single screw compressor with the straight line cross-section is chosen for the calculated example. In order to study the water pressure distribution on the gaterotor tooth flank, the pressure in the compression chamber volume and the relative sliding velocity of the rotor and the gaterotor at different ϕ_2 angles needs to be obtained firstly. This part of calculation process does not been introduced in this article. When the pressure and the relative velocity have been obtained, we can enter them in Fluent, and then calculated.

4. RESULTS

Pressure distribution along the tooth flank at different rotating angles of 0°, 20°, 42°and 55° of the tooth are respectively shown in Figure 5. The pressure in the upstream region of water film appears a wave crest which is located near the minimum width. The pressure in the downstream region appears negative value. The pressure distribution is different at different rotating angles of the gaterotor.
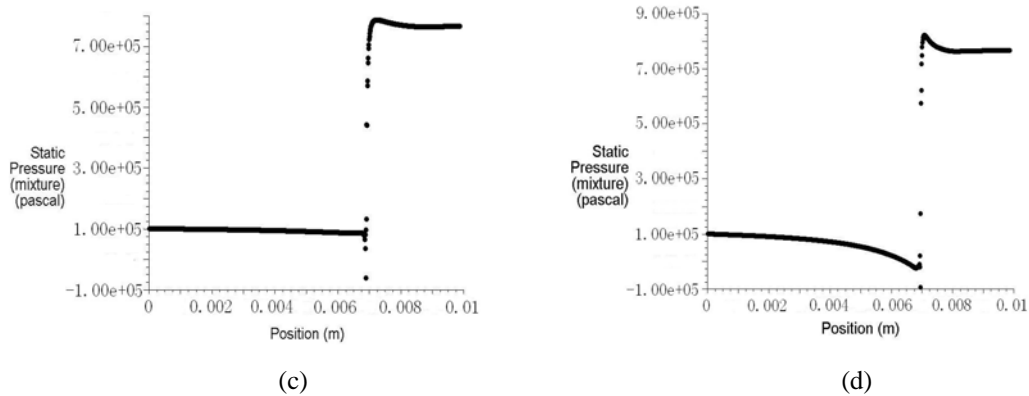

(a)

(b)

(c)

(d)
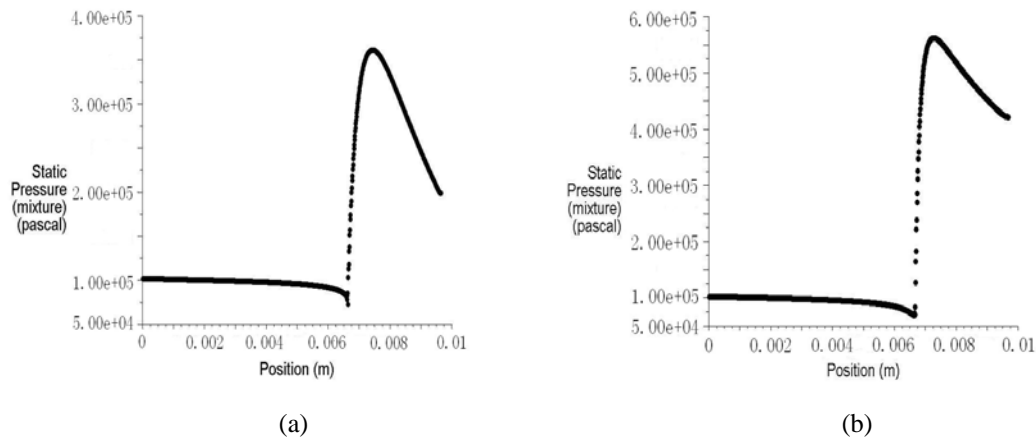
Figure 5: Pressure distribution at different rotating angles (ϕ_2)

(a) $\phi_2 = 0°$,(b) $\phi_2 = 20°$,(c) $\phi_2 = 42°$,(d) $\phi_2 = 55°$

According to the thermo physical properties of saturated water (e.g.,Shiming Yang, Wenquan Tao), saturated vapor pressure is 7381 Pascal at 313k. If the local pressure is lower than saturated vapor pressure, the gas nucleus will suddenly growing in water and the cavitation will occur. From Figure 5(a) and Figure 5(b), we can see that the local pressure is not low enough to make the weeny gas bubbles grow up. When the tooth rotates near the exhaust side, the minimum pressure has been lower than the standard atmospheric. In fact, such a low pressure does not exist in nature. These characteristics obviously prove the existence of the phenomenon of the cavitation. The pressure distribution at rotating angles of 42°and 55°are recalculated by using cavitation model, as shown in Figure 6.
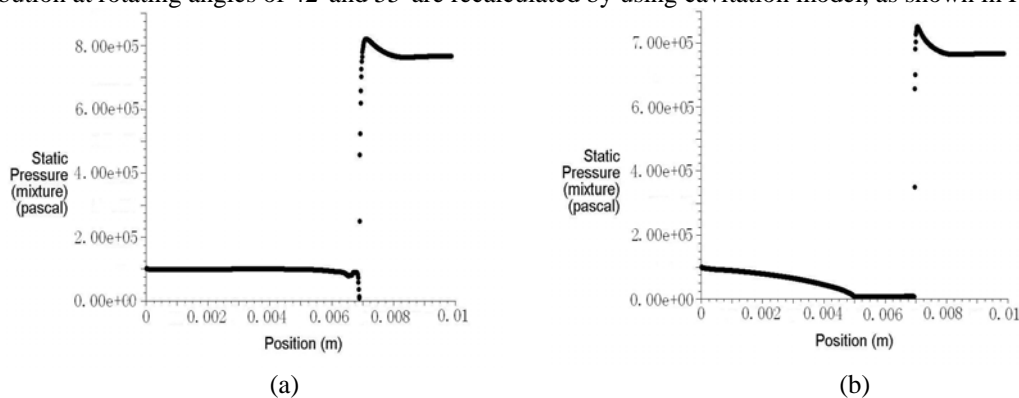

(a)

(b)

Figure 6: Pressure distributions at different rotating angles considering cavitation

(a) $\phi_2 = 42°$,(b) $\phi_2 = 55°$

(a)

(b)

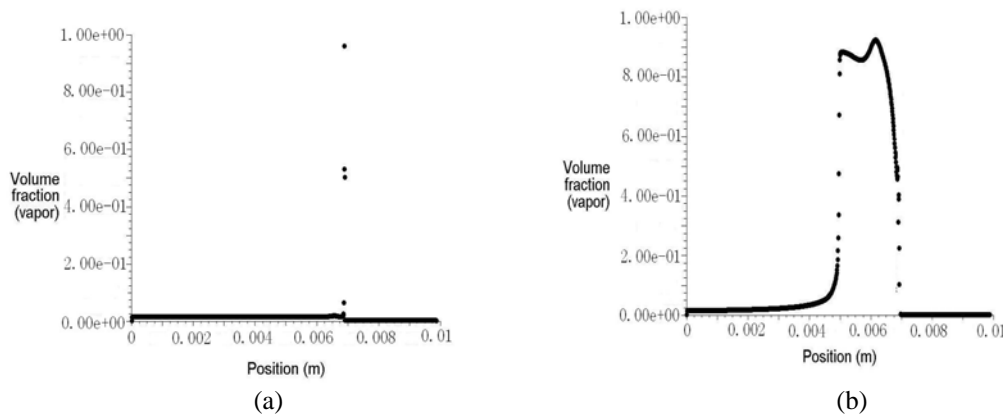**Figure 7:** Vapor volume fraction at different angles(ϕ_2)

(a) $\phi_2 = 42°$,(b) $\phi_2 = 55°$

When the cavitation model is adopted in the calculation of the water film force, the pressure distribution in the positive pressure area is basically identical with the result which is calculated by one-phase model, but the pressure distribution in the negative pressure area has a big difference. It is obviously incorrect that the water film force has became a negative value without considering cavitation. After using cavitation model in the calculation, the result has been modified effectively. The vapor volume fraction suddenly increasing and dropping means the generation and collapse of the bubble. As shown in Figure 7, in a single screw compressor with the straight line cross-section, cavitation usually occurs in the low pressure side of the contact line. With the gaterotor rotation angle increasing, the cavitation is more significant. Cavitation is greatly influenced by the shape of the lubrication geometry, the pressure in the compression chamber, and the relative sliding velocity. However, in a certain displacement of the single screw compressor, the variation ranges of the compression chamber pressure and the relative sliding velocity have been restricted. We can reduce the occurrence of cavitation by improving the tooth profile of the gaterotor.

5. CONCLUSION

In this paper, we calculated the pressure distribution of the water film along the tooth flank using one phase model and the cavitation model in a water flooded single screw compressor. The following conclusions can be obtained from the calculated results.

1. Possibility of negative pressure distribution is mainly effected by the profile of the clearance between the tooth flank and the groove blank. A convergent-divergent profile of the clearance increases the possibility of the existing of negative pressure distribution.
2. Negative pressure distribution of water film obtained by cavitation model is very different from that obtained by one phase model. When cavitation occurs, negative pressure distribution could be replaced by the saturated vapor pressure.
3. Positive pressure distribution obtained by the two models is almost same.

REFERENCES

Zimmern, B., and Patel, G. C., 1972, Design and Operating Characteristics of the Zimmern Single Screw Compressor, Compressor Technology Conference, Purdue, p. 96–99.
Post W., Zwaans M., 1986, Computer Simulation of the Hydrodynamic Lubrication in A Single Screw Compressor, Compressor Technology Conference, Purdue : p. 334-348.
Junfu Wang，2004，Computational Fluid Dynamics Analysis, Tsinghua University Press, Beijing, p. 121-122.
Shiming Yang, Wenquan Tao, Heat Transfer, Higher Education Press, Beijing, p.425.

ACKNOWLEDGMENT